Journal of ELECTRONIC MATERIALS, Vol. 46, No. 8, 2017
DOI: 10.1007/s11664-017-5500-2

Electromagnetic and Microwave Absorption Properties of Hybrid FeCrAl/Ti_3SiC_2 Composite in X-Band

YI LIU,[1,4] JIAJIA SI,[1] YUNYU LI,[1] FA LUO,[2] XIAOLEI SU,[1] JIE XU,[1] JUNBO WANG,[1] XINHAI HE,[1] and YIMIN SHI[3]

1.—Xi'an Polytechnic University, Xi'an 710048, People's Republic of China. 2.—Northwestern Polytechnical University, Xi'an 710072, People's Republic of China. 3.—Xi'an University of Architecture and Technology, Xi'an 710055, People's Republic of China. 4.—e-mail: yiliu1021@163.com

Hybrid magnetic–dielectric absorbers for electromagnetic applications consisting of FeCrAl and Ti_3SiC_2 powders have been fabricated by a ball-milling process and their electromagnetic characteristics and microwave absorption performance investigated in the frequency range from 8.2 GHz to 12.4 GHz. The dielectric loss increased with increasing Ti_3SiC_2 content, while the magnetic loss decreased. The electromagnetic parameters of the hybrid FeCrAl/Ti_3SiC_2 powders could be adjusted by adding various contents of Ti_3SiC_2. The hybrid powder with 20 wt.% Ti_3SiC_2 and 80 wt.% FeCrAl presented the most favorable microwave absorption performance. For the sample with thickness of 2.6 mm, effective absorption (< -10 dB) was obtained in the frequency range from 8.4 GHz to 12.1 GHz with a minimum value of -43.6 dB at 9.7 GHz. These results indicate that hybrid FeCrAl/Ti_3SiC_2 powders with appropriate weight ratio present better absorption performance than FeCrAl powder alone. This study makes a significant contribution to exploration of microwave absorption materials with low density, thin thickness, broad absorption bandwidth, and strong absorptivity.

Key words: FeCrAl/Ti_3SiC_2 hybrid powders, ball-milling process, electromagnetic characteristics, microwave absorption properties

INTRODUCTION

Electromagnetic (EM) waves are increasingly widely used with the rapid development of communication technology and high-frequency circuit devices operating in the GHz range. Although use of EM waves brings convenience to our daily life, the corresponding EM pollution and radiation have serious negative effects on commercial, industrial, and military systems.[1–4] Microwave absorption materials have been widely used to deal with these serious EM interference and pollution issues, because they can dissipate or shield EM waves effectively. Generally, microwave absorption materials consist of an insulating matrix containing absorbers that exhibit magnetic or dielectric loss. The insulating matrix provides bonding, while the absorber plays a key role in dissipating EM waves. Great attention has therefore been paid to absorbers with high absorptivity and wide absorption bandwidth, including carbon,[5] graphite,[6] SiC,[7] carbon nanotubes,[8] iron,[9–11] cobalt,[12,13] nickel,[14,15] metal alloys,[16–20] and ferrites.[21,22] However, individual absorbers exhibiting dielectric loss have narrow absorption bandwidth, while those showing magnetic loss are heavy, seriously limiting the application of such microwave absorption materials. To address these problems, researchers have focused on exploration of materials exhibiting both types of loss, i.e., dielectric and magnetic, to obtain absorbers with light weight, thin thickness, wide absorption bandwidth, and strong absorptivity. Mixing absorbers that exhibit dielectric and magnetic loss is an efficient way to adjust the resulting EM

(Received January 4, 2017; accepted April 1, 2017; published online April 14, 2017)

characteristics through the synergistic effect of the components, which can help to improve the absorption performance of microwave absorption materials.[23–25]

FeCrAl is a representative ferromagnetic alloy with excellent comprehensive mechanical and corrosion resistance properties as well as good chemical stability. Although the corrosion and oxidation behavior of FeCrAl powders have been widely investigated in previous work,[26,27] reports on their electromagnetic characteristics and microwave absorption performance are sparse. In recent work, we investigated the electromagnetic properties of FeCrAl powders. The results indicated that FeCrAl alloy shows obvious magnetic loss while its dielectric loss makes little contribution to dissipation of EM waves. Moreover, the high density (8.9 g/cm^3) of FeCrAl alloy is contrary to the tendency to explore lightweight microwave absorption materials. So, mixing a low-density absorber showing high dielectric loss with FeCrAl is an effective way to improve the electromagnetic performance of the alloy powder. Ti_3SiC_2 is a representative ternary compound with high electrical conductivity ($4.5 \times 10^6\ \Omega^{-1}\ m^{-1}$), low density (4.52 g/cm^3), and excellent chemical stability.[28–31] These merits make it a promising absorber for use in microwave absorption materials. The dielectric and microwave absorption properties of Ti_3SiC_2 powders and its compounds have been studied.[32–34] The results demonstrated that absorbers containing Ti_3SiC_2 powders present excellent microwave absorption performance in X-band. These excellent dielectric characteristics of Ti_3SiC_2 and outstanding magnetic qualities of FeCrAl motivate investigation of the electromagnetic and microwave absorption properties of hybrid FeCrAl/Ti_3SiC_2 powders. The results may contribute to development of microwave absorption materials with light weight, thin thickness, wide absorption bandwidth, and strong absorptivity.

In this study, different amounts of Ti_3SiC_2 were mixed with FeCrAl alloy powder using a ball-milling process. The influence of the Ti_3SiC_2 content on the electromagnetic characteristics of the resulting hybrid FeCrAl/Ti_3SiC_2 powders was studied. The microwave absorption of the hybrid powders was also investigated and optimized.

EXPERIMENTAL PROCEDURES

Commercially available spherical FeCrAl (75% Fe, 20% Cr, 5% Al) powder with particle size of 10 μm to 50 μm was purchased from Hunan Metallurgy Material Institute, China. Ti_3SiC_2 powder was obtained by ball milling as-prepared loose bulk synthesized by solid reaction route at high temperature, with average particle size of about 5 μm. To obtain homogeneous hybrid powders, FeCrAl and Ti_3SiC_2 powders were ball-milled for 6 h. Microwave absorption materials were prepared by mixing the hybrid powders with paraffin as a nearly EM-wave-transparent matrix. The total content of the fillers in the paraffin matrix was fixed at 60 wt.%, while the mass ratio of FeCrAl to Ti_3SiC_2 was 1:0, 9:1, 8:2, and 7:3 in sample 1, 2, 3, and 4, respectively.

The phase composition of the powders was determined using Cu K_α radiation (X-Pert Diffractometer, Philips, The Netherlands). The morphology of the powders was observed by scanning electron microscopy (Tescan China, Ltd., Shanghai, Tescan VEGA3 SBH). The complex permittivity and permeability were measured in the frequency range from 8.2 GHz to 12.4 GHz by the rectangle waveguide method using a vector network analyzer (Agilent Technologies E8362B, 10 MHz to 20 GHz). The samples were prepared by thoroughly mixing the powders with molten paraffin matrix, then pouring the homogeneous mixture in flow state into a flange and cooling at room temperature. Each tested specimen had length of 22.86 mm, width of 10.16 mm, and thickness of 2.58 mm after removal from the flange. The reflection loss of each single-layer sample was calculated using transmission-line theory based on measured electromagnetic parameters via the following equations[35–37]:

$$\mathrm{RL\ (dB)} = 20\log\left|{}^{(Z_{in}-Z_0)}\!/_{(Z_{in}+Z_0)}\right|, \quad (1)$$

$$Z_0 = \sqrt{{}^{\mu_0}\!/_{\varepsilon_0}}, \quad (2)$$

$$Z_{in} = Z_0\sqrt{{}^{\mu_r}\!/_{\varepsilon_r}}\tanh\left[j\frac{2\pi}{c}\sqrt{\mu_r\varepsilon_r}fd\right], \quad (3)$$

where Z_{in} and Z_0 are the input impedance of the absorber and free space, respectively, ε_r and μ_r are the relative complex permittivity and permeability, f is the frequency, d is the thickness, and c is the speed of light.

RESULTS AND DISCUSSION

The XRD spectra of the commercial FeCrAl, as-prepared Ti_3SiC_2, and hybrid FeCrAl/Ti_3SiC_2 powders are shown in Fig. 1. The diffraction peaks of crystalline a-Fe are observed in Fig. 1a, located at 2θ values of 44.4°, 64.6°, and 81.8°, corresponding to (110), (200), and (211) crystal planes, respectively. In Fig. 1b, the diffraction peak of TiC is identified, besides the main crystal phase Ti_3SiC_2. TiC forms as a secondary phase during synthesis of Ti_3SiC_2 and is difficult to eliminate completely. The mass ratio of Ti_3SiC_2 was 96.3 wt.%, calculated by the experimental equation. After the ball-milling process, no other phases were identified in the hybrid powders except FeCrAl and Ti_3SiC_2, as shown in Fig. 1c. This result indicates that no reactions occurred between the FeCrAl and Ti_3SiC_2 powders during the ball-milling process.

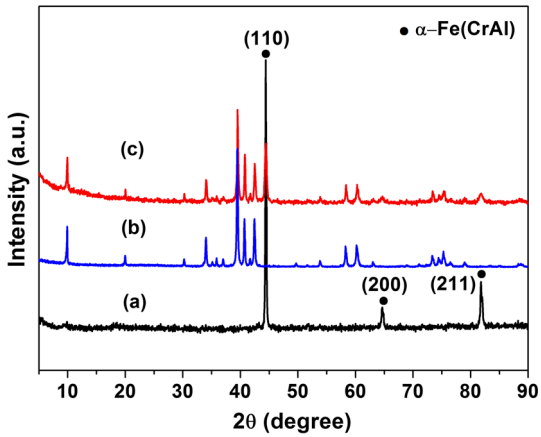

Fig. 1. XRD patterns of (a) commercial FeCrAl powder, (b) as-prepared Ti_3SiC_2, and (c) hybrid FeCrAl/Ti_3SiC_2 powders.

Figure 2 shows the morphology of the commercial FeCrAl, as-prepared Ti_3SiC_2, and hybrid FeCrAl/Ti_3SiC_2 powders. As seen from Fig. 2a, the initial FeCrAl powder was spherical with wide particle size distribution of 5 μm to 50 μm. The as-prepared Ti_3SiC_2 powder presented irregular shape with particle size distribution of 2 μm to 10 μm, as shown in Fig. 2b. After the ball-milling process, the spherical FeCrAl particles transformed to flaky shape with increased plane size and decreased thickness, as shown in Fig. 2b–d. In addition, the FeCrAl and Ti_3SiC_2 powders were homogeneously mixed with no obvious agglomeration in the hybrid powders. For microwave absorption materials consisting of a lossy absorber and an insulating matrix, the electromagnetic performance is strongly influenced by the content as well as characteristics of the absorber. With increasing milling time, the aspect

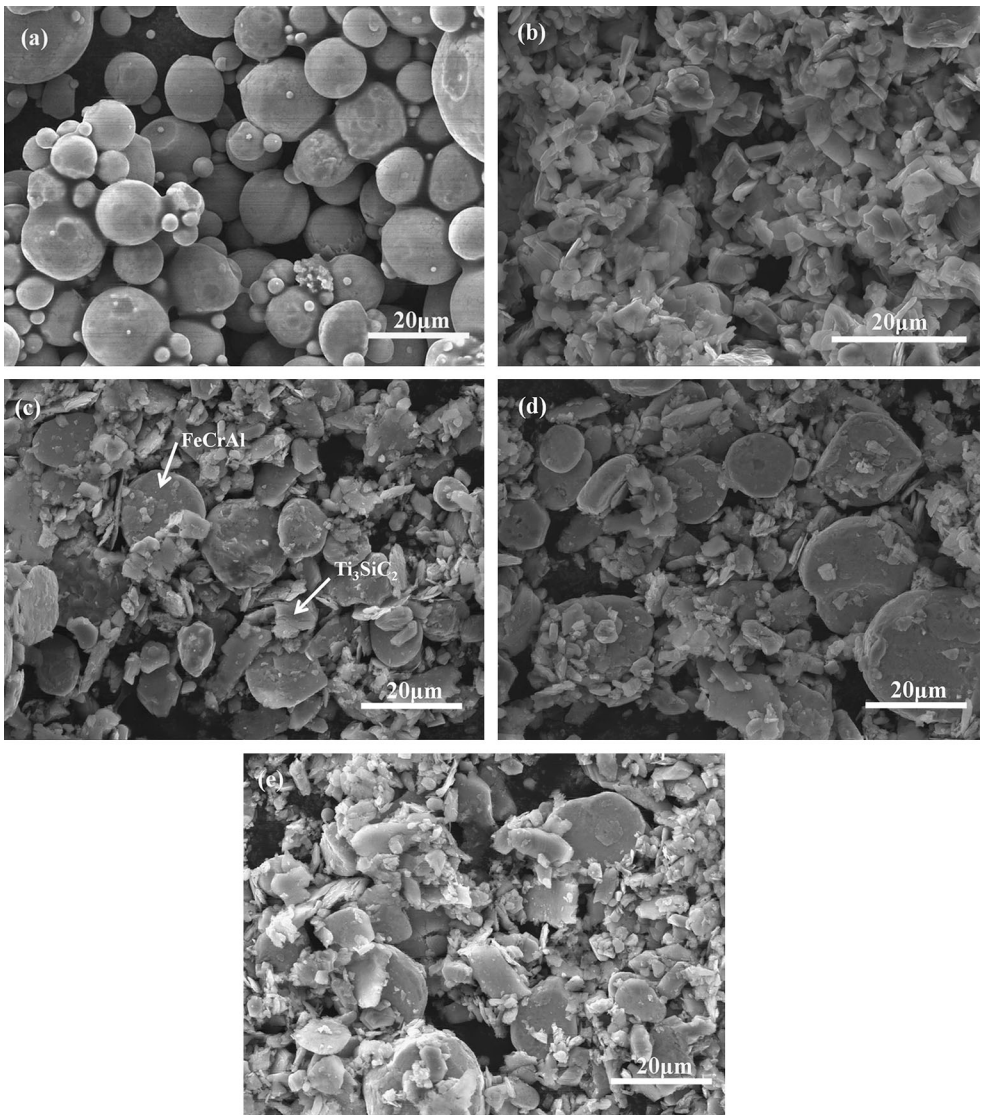

Fig. 2. Morphology of raw FeCrAl, Ti_3SiC_2, and hybrid FeCrAl/Ti_3SiC_2 powders: (a) sample 1, (b) Ti_3SiC_2, (c) sample 2, (d) sample 3, and (e) sample 4.

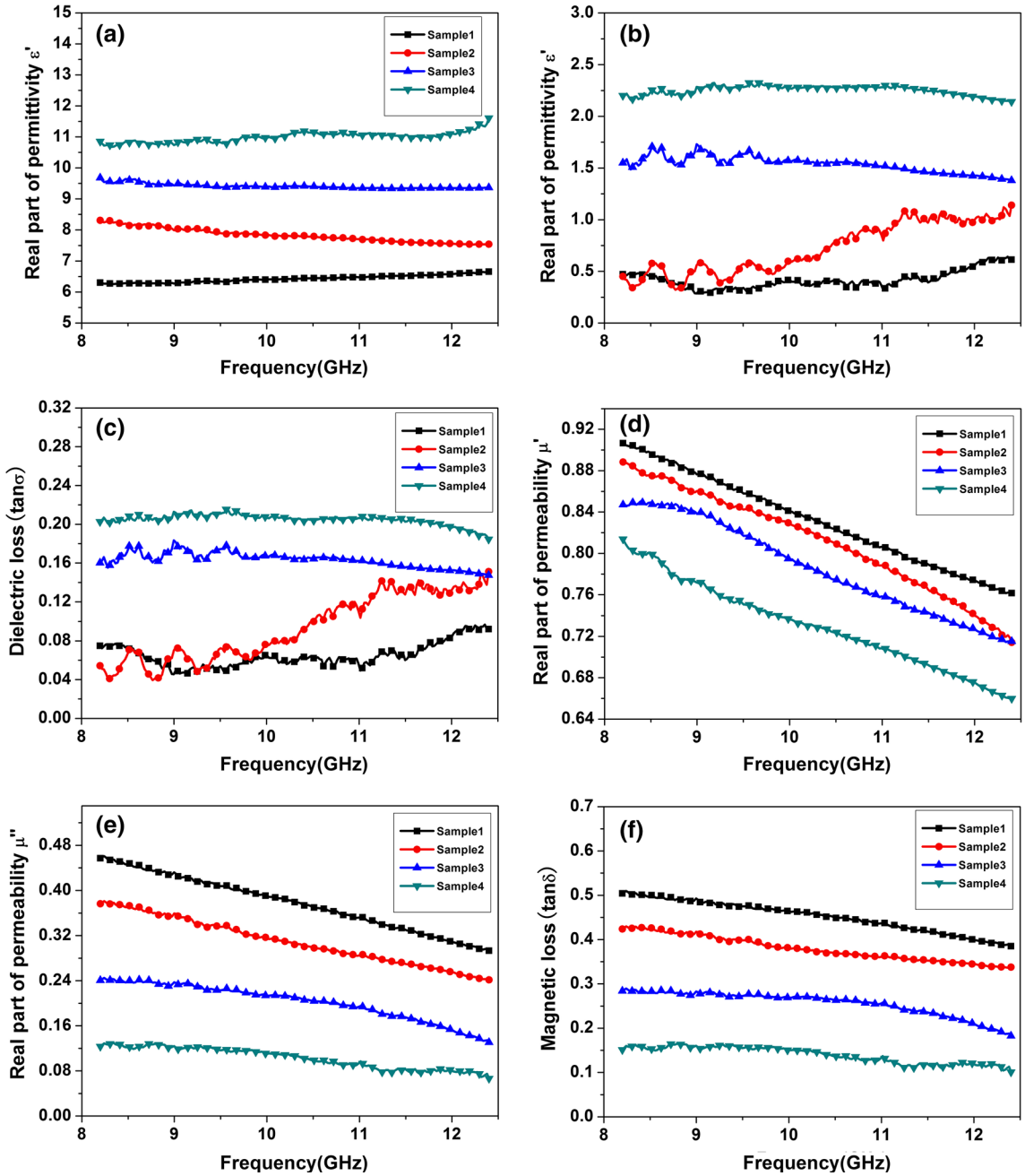

Fig. 3. Frequency dependence of complex permittivity and permeability in frequency range from 8.2 GHz to 12.4 GHz: (a) real part of complex permittivity ε', (b) imaginary part of complex permittivity ε'', (c) dielectric loss tan σ, (d) real part of complex permeability μ', (e) imaginary part of complex permeability μ'', and (f) magnetic loss tan δ.

ratio of the as-milled FeCrAl particles was enhanced. This will suppress eddy currents in high-frequency electromagnetic fields, which is closely related to improved electromagnetic and microwave absorption properties.

The electromagnetic properties of a microwave absorption material can be characterized based on its complex permittivity ($\varepsilon = \varepsilon' - j\varepsilon''$) and permeability ($\mu = \mu' - j\mu''$). The real parts of the complex permittivity (ε') and permeability (μ') represent the storage capacity of the absorber, while the imaginary parts (ε'' and μ'') represent its lossy ability.[38]

Figure 3 shows the frequency dependence of the complex permittivity and permeability in the frequency range from 8.2 GHz to 12.4 GHz. As seen from Fig. 3a–c, the real and imaginary parts for the individual FeCrAl powders lay in the ranges of 5.76 to 6.60 and 0.04 to 0.44, respectively, while the dielectric loss was below 0.1. This low complex permittivity and dielectric loss indicate that dielectric loss will make little contribution to dissipation of electromagnetic waves. When the Ti_3SiC_2 content was increased from 0 wt.% to 30 wt.%, both the complex permittivity and dielectric loss increased.

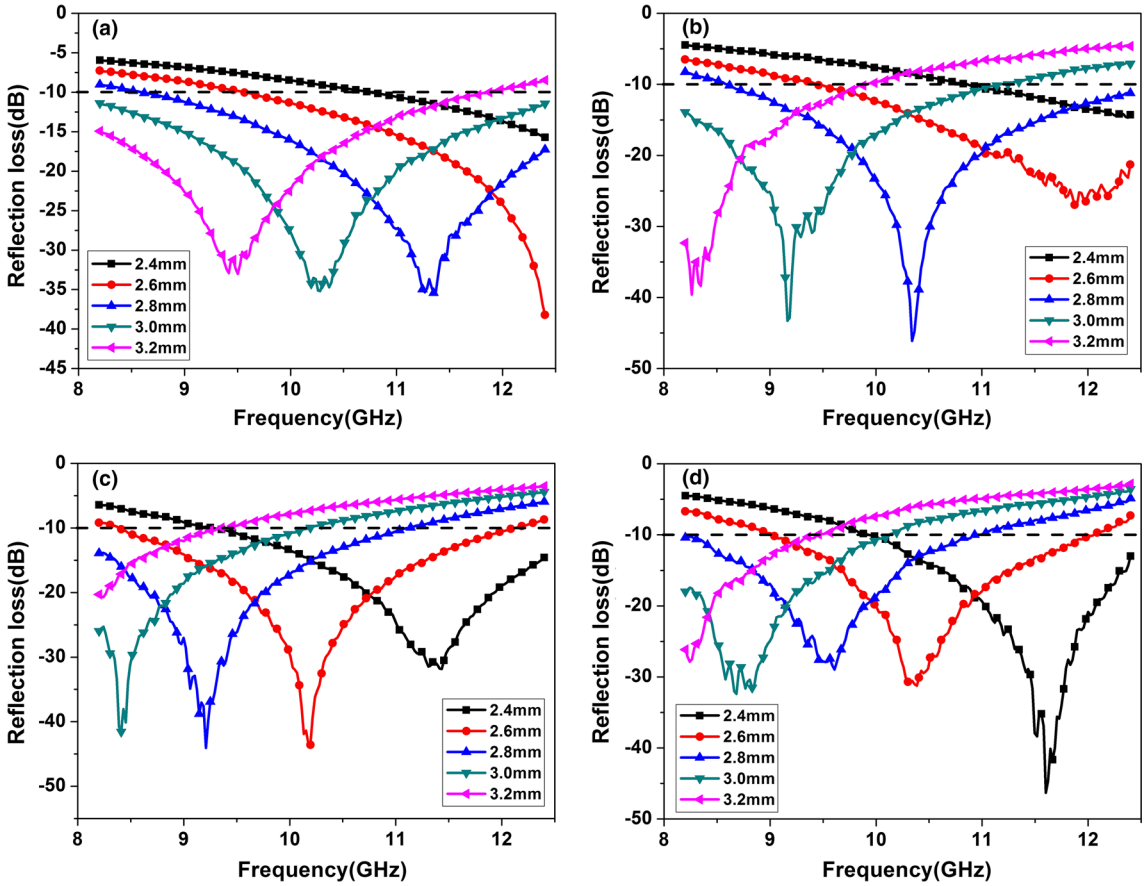

Fig. 4. Reflection loss (RL) of samples with different Ti_3SiC_2 contents calculated based on transmission-line theory: (a) sample 1, (b) sample 2, (c) sample 3, and (d) sample 4.

Table I. Microwave absorption performance of hybrid FeCrAl/Ti_3SiC_2 powders with different Ti_3SiC_2 contents

Sample	Components	Effective bandwidth (GHz)	Minimum RL value (dB)	Thickness (mm)
Sample 1	Raw FeCrAl	8.2–12.4	−18.9	3.0
Sample 2	90 wt.% FeCrAl + 10 wt.% Ti_3SiC_2	8.6–12.4	−46.1	2.8
Sample 3	80 wt.% FeCrAl + 20 wt.% Ti_3SiC_2	8.4–12.1	−43.6	2.6
Sample 4	70 wt.% FeCrAl + 30 wt.% Ti_3SiC_2	9–12	−31.2	2.6

For sample 4, containing 30 wt.% Ti_3SiC_2, the real and imaginary part of the complex permittivity reached 10.8 to 11.6 and 2.2 to 2.3, while the dielectric loss rose to 0.2. As stated above, Ti_3SiC_2 is a ternary layered compound with excellent electrical conductivity. Conductive loss plays a key role in dissipating EM waves when Ti_3SiC_2 powder is dispersed in an insulating matrix. So, the dielectric performance of the hybrid powders was improved when some of the FeCrAl powder was replaced by the same content of Ti_3SiC_2.

Figure 3d–f shows the complex permeability and magnetic loss in the frequency range from 8.2 GHz to 12.4 GHz. It can be seen that the complex permeability declined with increasing frequency. This obvious dispersion effect contributes to broadened absorption bandwidth and strengthened absorptivity of electromagnetic waves. The complex permeability and magnetic loss for the FeCrAl powder alone were higher than for the hybrid powders due to its outstanding magnetic characteristics. As the Ti_3SiC_2 content was increased from 0 wt.% to 30 wt.%, the real part of the complex permeability decreased from 0.9 to 0.76 to become 0.81 to 0.66, while the imaginary part declined from 0.46 to 0.29 to become 0.12 to 0.06. The magnetic characteristics of the hybrid Ti_3SiC_2/FeCrAl powders were mainly dominated by those of FeCrAl, because Ti_3SiC_2 is a nonmagnetic material. Therefore, increasing the Ti_3SiC_2 content in the hybrid

Table II. Comparison of hybrid FeCrAl/Ti_3SiC_2 with some other composites

Sample	Minimum RL value (dB)	RL < −10 dB (GHz)	Matching thickness (mm)	Ref.
FeCrAl/Ti_3SiC_2	−43.6	8.4–12.1	2.6	This study
Fe_3O_4/MnO_2	−20.1	8.5–11.7	2.0	39
$Fe_{50}Ni_{50}$/RGO	−23.9	8.8–12.4	3.0	40
Fe_3O_4/CuPc	−28.9	8.2–10.2	3.2	41
$La_{0.7}Sr_{0.3}MnO_3/C$	−12.3	8.5–9.2	4.0	42
$Ni_{0.6}Zn_{0.4}Fe_2O_4$/PANI	−30.5	8.2–11.6	3.5	43
$Li_{0.4}Mg_{0.6}Fe_2O_4/TiO_2$	−41.6	9.46–11.3	2.5	44
Ni/C	−12.8	8.2–10.7	2.2	45

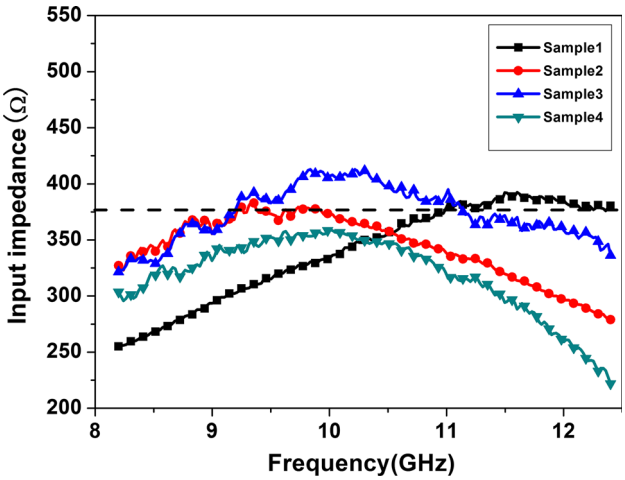

Fig. 5. Input impedance of samples with different Ti_3SiC_2 contents and thickness of 2.6 mm.

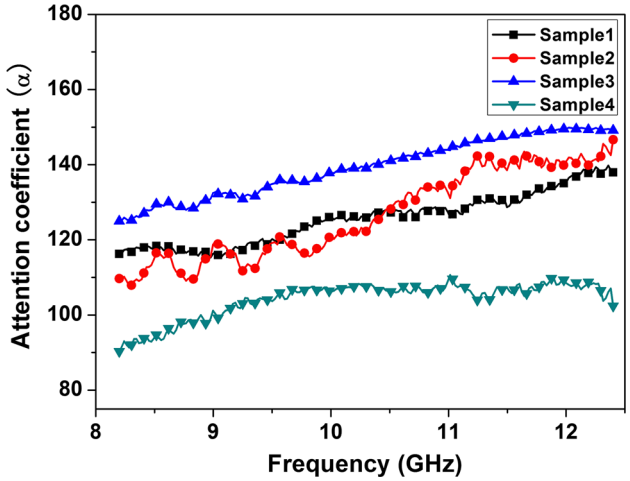

Fig. 6. Calculated attenuation constants for samples with different Ti_3SiC_2 contents.

powders resulted in reduced complex permeability and magnetic loss.

The reflection loss (RL) is a parameter that characterizes the absorption performance of microwave absorption materials. The RL of the samples was calculated based on transmission-line theory, and the results are shown in Fig. 4. All the reflection loss peaks shifted toward lower frequency range as the thickness was increased from 2.4 mm to 3.2 mm. The relationship between the matching frequency and thickness can be illustrated as follows[34,38]:

$$f_m = {}^{c}/_{4d_m} \cdot {}^{1}/_{\sqrt{\varepsilon'\mu'}} \cdot \left(1 + \tan^2 {}^{\delta}/_{8}\right)^{-1}, \qquad (4)$$

where f_m and d_m are the matching frequency and thickness, respectively, and c is the speed of light. It is reasonable that the matching frequency decreases with increasing thickness for given sample composition.

The microwave absorption performance of the individual FeCrAl and hybrid FeCrAl/Ti_3SiC_2 powders is presented in Table I. For sample 1 with thickness of 3.0 mm, the effective absorption bandwidth (<−10 dB) covered the whole X-band with minimum value of −35.2 dB at 10.3 GHz. When 10 wt.% Ti_3SiC_2 was added into the hybrid powder, effective absorption was obtained from 8.6 GHz to 12.4 GHz, with minimum RL value of −46.1 dB at 10.3 GHz. Although the effective absorption bandwidth become narrow, the thickness of the sample was decreased to 2.8 mm. As discussed above, FeCrAl is a magnetic alloy with high magnetic loss, and the absorption mechanism is mainly attributed to eddy current loss and magnetic resonance loss. Meanwhile, Ti_3SiC_2 exhibits outstanding dielectric loss, so increasing the Ti_3SiC_2 content resulted in enhanced polarization and conductance loss. The decreased thickness of the samples containing the hybrid Ti_3SiC_2/FeCrAl powders is ascribed to the synergistic effect of dielectric and magnetic loss. When 20 wt.% FeCrAl was replaced by Ti_3SiC_2, the minimum RL value reached −43.6 dB and effective absorption was obtained from 8.4 GHz to 12.1 GHz. The optimum thickness for the sample decreased to 2.6 mm. It was observed that sample 3 presented the most favorable microwave absorption performance with the thinnest thickness. On further increasing the Ti_3SiC_2 content to 30 wt.%, the RL value increased while the effective absorption

bandwidth became narrow. For microwave absorption materials, the impedance must match that of free space so that incident waves can enter and be attenuated in the material.[38] The impedance of the sample containing 30 wt.% Ti_3SiC_2 deviated from this matching condition, so incident waves were strongly reflected from the surface of the sample, resulting in poor absorption performance. A comparison of the hybrid Ti_3SiC_2/FeCrAl powders with some other composites, such as Fe_3O_4/MnO_2,[39] $Fe_{50}Ni_{50}$/reduced graphene oxide (RGO),[40] Fe_3O_4/copper phthalocyanine (CuPc),[41] $La_{0.7}Sr_{0.3}MnO_3$/C,[42] $Ni_{0.6}Zn_{0.4}Fe_2O_4$/polyaniline (PANI),[43] $Li_{0.4}Mg_{0.6}Fe_2O_4/TiO_2$,[44] and Ni/C,[45] is presented in Table II. The effective absorption bandwidth of the hybrid Ti_3SiC_2/FeCrAl was the widest and its reflection loss the lowest. These results indicate that such Ti_3SiC_2/FeCrAl composites could represent promising microwave absorption materials for use in practical applications.

To elucidate the dissipation mechanism, the input impedance of the samples was calculated and analyzed. Figure 5 shows the input impedance of the samples with thickness of 2.6 mm. It can be seen that the input impedance increased as the Ti_3SiC_2 content was increased from 0 wt.% to 20 wt.%, while it declined when the Ti_3SiC_2 content reached 30 wt.%. To obtain excellent absorption performance, the impedance of a microwave absorption material must meet the matching condition so that incident waves can enter the materials and be attenuated. As the Ti_3SiC_2 content was increased from 0 wt.% to 20 wt.%, the impedance of the sample approached that of free space, which will result in greater penetration of electromagnetic waves into the material to be dissipated, leading to improved microwave absorption performance. The impedance value of sample 3 was closest to 377 Ω, resulting in the most favorable microwave absorption performance. On further increasing the Ti_3SiC_2 content to 30 wt.%, the deviation of the impedance from the matching condition caused strong reflection of incident waves, resulting in poor absorption performance.

The dissipation ability of microwave absorption materials is characterized by the attenuation constant, which can be expressed as follows[11]:

$$\alpha = \frac{\sqrt{2}\pi f}{c}\sqrt{\mu''\varepsilon'' - \mu'\varepsilon' + \sqrt{(\mu'^2 + \mu''^2)(\varepsilon'^2 + \varepsilon''^2)}}. \quad (5)$$

where α is the attenuation constant, f is the frequency, c is the speed of light. The calculated attenuation constants for the samples are shown in Fig. 6. The attenuation constant first increased then decreased with rising Ti_3SiC_2 content, and the sample with 20 wt.% Ti_3SiC_2 showed the highest attenuation constant value. The attenuation constant of the raw FeCrAl powder was 81 neper per meter (Np/m) to 108 Np/m, while it reached 125 Np/m to 149 Np/m when the Ti_3SiC_2 content was increased to 20 wt.%. The larger the attenuation constant value, the greater the dissipation of electromagnetic waves. On further increasing the Ti_3SiC_2 content to 30 wt.%, the attenuation constant value decreased to 90 Np/m to 102 Np/m, resulting in degraded microwave absorption performance.

CONCLUSIONS

The electromagnetic and microwave absorption properties of hybrid Ti_3SiC_2/FeCrAl powders were investigated. The electromagnetic parameters of the hybrid powders could be adjusted by adding various contents of Ti_3SiC_2. The complex permittivity increased while the complex permeability declined with rising Ti_3SiC_2 content. The sample with 20 wt.% Ti_3SiC_2 presented the most favorable microwave absorption performance. Effective absorption (< -10 dB) was obtained in the frequency range from 8.4 GHz to 12.1 GHz for the sample with thickness of 2.6 mm, with minimum RL value of −43.6 dB at the matching frequency of 9.7 GHz.

ACKNOWLEDGEMENTS

This work was supported by the PhD Start-Up Fund of XPU (BS1615 and BS1612), State Key Laboratory of Solidification Processing in NWPU (No. SKLSP201637), Shaanxi Natural Science Foundation (No. 2013JM6008), Shaanxi Provincial Science and Technology Department (No. 2014JM2-5066), and Shaanxi Industrial Science and Technology Research Project (No. 2016GY-014).

REFERENCES

1. Y. Kato, S. Sugimoto, K.I. Shinohara, N. Tezuka, T. Kagotani, and K. Inomata, *Mater. Trans. JIM* 43, 408 (2002).
2. P. Saini, V. Choudhary, B. Singh, R. Mathur, and S. Dhawan, *Mater. Chem. Phys.* 113, 923 (2009).
3. F. Qin and C. Brosseau, *J. Appl. Phys.* 111, 061301 (2012).
4. B. Wang, J. Zhang, T. Wang, L. Qiao, and F. Li, *J. Alloys Compd.* 567, 24 (2013).
5. D.L. Zhao and Z.M. Shen, *Mater. Lett.* 62, 3705 (2008).
6. Y. Fan, H. Yang, M. Li, and G. Zou, *Mater. Chem. Phys.* 115, 697 (2009).
7. A. Kumar, V. Agarwala, and D. Singh, *Ceram. Int.* 40, 1801 (2014).
8. X. Qi, Y. Yang, W. Zhong, Y. Deng, C. Au, and Y. Du, *J. Solid State Chem.* 182, 2695 (2009).
9. X. Liu, D. Geng, H. Meng, P. Shang, and Z. Zhang, *Appl. Phys. Lett.* 92, 173117 (2008).
10. X. Zhang, X. Dong, H. Huang, B. Lv, J. Lei, and C. Choi, *J. Phys. D Appl. Phys.* 40, 5383 (2007).
11. X.T. Chu, B.N. Ta, L.T.H. Ngo, M.H. Do, P.X. Nguyen, and D.N.H. Nam, *J. Electron. Mater.* 45, 2313 (2016).
12. Q. Liu, D. Zhang, and T. Fan, *Appl. Phys. Lett.* 93, 3110 (2008).
13. Z. Zheng, B. Xu, L. Huang, L. He, and X. Ni, *Solid State Sci.* 10, 318 (2008).
14. X. Zhang, X. Dong, H. Huang, Y. Liu, W. Wang, X. Zhu, B. Lv, J. Lei, and C. Lee, *Appl. Phys. Lett.* 89, 3115 (2006).
15. B. Gao, L. Qiao, J. Wang, Q. Liu, F. Li, J. Feng, and D. Xue, *J. Phys. D Appl. Phys.* 41, 235005 (2008).
16. X. Li, X. Han, Y. Tan, and P. Xu, *J. Alloys Compd.* 464, 354 (2008).
17. Y. Feng and T. Qiu, *J. Alloys Compd.* 513, 458 (2012).

18. L.C. Cheng, J.L. Xiong, H.Y. Zhou, S.K. Pan, and H.H. Huang, *J. Electron. Mater.* 45, 1025 (2016).
19. Z.Q. Qiao, S.K. Pan, J.L. Xiong, L.C. Cheng, P.H. Lin, and J.L. Luo, *J. Electron. Mater.* 46, 664 (2017).
20. S.C. Gu, Y.P. Duan, P. Duan, S. Wang, G.P. Qiu, and Y.Z. Liu, *J. Electron. Mater.* 44, 2335 (2015).
21. S. Abbas, A. Dixit, R. Chatterjee, and T. Goel, *J. Magn. Magn. Mater.* 309, 23 (2007).
22. A. Ohlan, K. Singh, A. Chandra, and S. Dhawan, *Appl. Phys. Lett.* 93, 053117 (2008).
23. Z. Zhu, X. Sun, G. Li, H. Xue, H. Guo, X. Fan, X. Pan, and J. He, *J. Magn. Magn. Mater.* 377, 101 (2015).
24. L. Liu, Y. Duan, L. Ma, S. Liu, and Z. Yu, *Appl. Surf. Sci.* 257, 845 (2010).
25. F. Wen, F. Zhang, J. Xiang, W. Hu, S. Yuan, and Z. Liu, *J. Magn. Magn. Mater.* 343, 283 (2013).
26. C. Badini and F. Laurella, *Surf. Coat. Technol.* 135, 296 (2001).
27. R. Fetzer, A. Weisenburger, A. Jianu, and G. Müller, *Corros. Sci.* 55, 215 (2012).
28. M.W. Barsoum and T. El-Raghy, *J. Am. Ceram. Soc.* 79, 1955 (1996).
29. C. Racault, F. Langlais, and R. Naslain, *J. Mater. Sci.* 29, 3387 (1994).
30. Y. Zhou and Z. Sun, *J. Mater. Sci.* 35, 4345 (2000).
31. F. Sato, J.F. Li, and R. Watanabe, *Mater. Trans. JIM* 41, 607 (2000).
32. Y. Liu, F. Luo, W. Zhou, and D. Zhu, *J. Alloys Compd.* 576, 46 (2013).
33. Y. Liu, F. Luo, J. Su, W. Zhou, D. Zhu, and Z. Li, *J. Alloys Compd.* 619, 857 (2015).
34. Y. Liu, F. Luo, J. Su, W. Zhou, and D. Zhu, *J. Electron. Mater.* 44, 870 (2015).
35. M.S. Cao, W.L. Song, Z.L. Hou, B. Wen, and J. Yuan, *Carbon* 48, 790 (2010).
36. C. Qiang, J. Xu, Z. Zhang, L. Tian, S. Xiao, Y. Liu, and P. Xu, *J. Alloys Compd.* 506, 96 (2010).
37. Y. Qing, W. Zhou, S. Jia, F. Luo, and D. Zhu, *Appl. Phys. A* 100, 1179 (2010).
38. Y. Liu, F. Luo, J. Su, W. Zhou, and D. Zhu, *J. Magn. Magn. Mater.* 365, 129 (2014).
39. M. Qiao, X. Lei, Y. Ma, L. Tian, K. Su, and Q. Zhang, *Chem. Eng. J.* 304, 558 (2016).
40. J. Wang, J. Wang, R. Xu, Y. Sun, B. Zhang, W. Chen, T. Wang, and S. Yang, *J. Alloys Compd.* 653, 19 (2015).
41. Z. Ma, R. Zhao, X. Yang, J. Wei, F. Meng, X. Liu, Z. Ma, R. Zhao, X. Yang, and J. Wei, *Mater. Lett.* 69, 31 (2012).
42. C.Y. Tsay, Y.H. Huang, and D.S. Hung, *Ceram. Int.* 40, 3950 (2014).
43. M. Wang, G. Ji, B. Zhang, D. Tang, Y. Yang, and Y. Du, *J. Magn. Magn. Mater.* 377, 56 (2015).
44. P. Bhattacharya, G. Hatui, A. Mandal, C.K. Das, R. Kumar, and T.C. Shami, *J. Alloys Compd.* 590, 337 (2014).
45. V. Sunny, D.S. Kumar, P. Mohanan, and M.R. Anantharaman, *Mater. Lett.* 64, 1131 (2010).